

## NEWS ABOUT $\nu$ 'S

E.K. AKHMEDOV

*Centro de Física das Interações Fundamentais (CFIF)*

*Departamento de Física, Instituto Superior Técnico*

*Av. Rovisco Pais, P-1049-001 Lisboa, Portugal*

**Abstract.** We review new results in neutrino physics, including the latest data of the Super-Kamiokande, SNO and K2K experiments.

### 1. Introduction

The recent evidence for neutrino oscillations [1] provided us with the first firm evidence of physics beyond the standard model and opened a new and exciting era in neutrino studies. Neutrino physics is a very active branch of particle physics now, both experimentally and theoretically. The experimental data keep pouring in, and new experiments are either under way or in an advanced stage of planning. On the theoretical side, there are new analyses of the data, both in the 3-flavour and 4-flavour schemes; the analyses of the solar neutrino data are being extended to cover the “dark side” of the parameter space, not studied (or little studied) before; the reach of future planned experiments is being investigated and new experiments designed to eliminate the white spots on the map of neutrino properties are being suggested. In addition, since the discovery of neutrino oscillations a large number of models of neutrino mass was proposed and some old models were reconsidered in the light of the new data.

In the present lectures we review new results in neutrino physics, mainly the experimental ones. We discuss the latest results of the solar and atmospheric neutrino experiments and their analyses; results from the reactor and accelerator experiments, including those from the first long-baseline accelerator neutrino experiment K2K, and then briefly discuss future experiments and projects. Finally, we discuss how all the presently available data can be summarized concisely in terms of the phenomenologically allowed structures of the neutrino mass matrix.

We do not discuss neutrino mass model because of the lack of space; for recent reviews on this subject the reader is referred to [2, 3, 4, 5, 6, 7].

The data reviewed in the lectures given at the NATO ASI in Cascais included the results reported at the Neutrino 2000 Conference in Sudbury, June 16 - 21, 2000. However, the present written version is updated to include the results reported up to November of 2000. For other recent reviews on neutrino physics see, e.g., [8, 9].

## 2. General properties of neutrinos

Direct kinematic searches of neutrino masses yield the following upper limits [10, 11, 12, 13]:

$$m_{\nu_1} < 2.5 \text{ eV at 95\% c.l. (Troitsk)}; < 2.2 \text{ eV at 95\% c.l. (Mainz)}; \quad (1)$$

$$m_{\nu_2} < 170 \text{ keV at 90\% c.l. (PSI; } \pi^+ \rightarrow \mu^+ + \nu_\mu); \quad (2)$$

$$m_{\nu_3} < 15.5 \text{ MeV at 95\% c.l. (ALEPH, CLEO, OPAL; } \tau \text{ decays)}. \quad (3)$$

Here  $\nu_1$ ,  $\nu_2$  and  $\nu_3$  are assumed to be the primary mass components of  $\nu_e$ ,  $\nu_\mu$  and  $\nu_\tau$ , respectively. However, since we know now that at least one mixing angle in the lepton sector is large, these limits may need a re-interpretation. In particular, the upper bound on  $m_{\nu_3}$  may in fact be much more stringent than the one in eq. (3).

How many neutrino species are there? Electron and muon neutrinos have been known to exist since 1955 and 1964, respectively. Although there were strong theoretical and indirect experimental reasons to believe that there exist the third neutrino species,  $\nu_\tau$ , until recently it was not unambiguously experimentally detected. In July of 2000 the DONUT Collaboration reported the direct experimental evidence for  $\nu_\tau$  [14].

Are there any more neutrino species? The number of the types of the standard neutrinos can be found from the  $Z^0$  decay width. Indeed, neutrinos from the  $Z^0$  decays are not detected, and therefore the difference between the measured total width of the  $Z^0$  boson and the sum of its partial widths of decay into quarks and charged leptons, the so-called invisible width,  $\Gamma_{inv} = \Gamma_{tot} - \Gamma_{vis} = 498 \pm 4.2 \text{ MeV}$ , should be due to the decay into  $\nu\bar{\nu}$  pairs. Taking into account that the partial width of  $Z^0$  decay into one  $\nu\bar{\nu}$  pair  $\Gamma_{\nu\bar{\nu}} = 166.9 \text{ MeV}$  one finds the number of the light active neutrino species [12]:

$$N_\nu = \frac{\Gamma_{inv}}{\Gamma_{\nu\bar{\nu}}} = 2.994 \pm 0.012, \quad (4)$$

in a very good agreement with the existence of the three neutrino flavours. There are also indirect limits on the number of light ( $m < 1 \text{ MeV}$ ) neutrino species (including possible electroweak singlet, i.e. "sterile" neutrinos  $\nu_s$ )

coming from big bang nucleosynthesis. The number of neutrino species in equilibrium with the rest of the universe at the nucleosynthesis epoch is

$$N_\nu < 3.3, \quad (5)$$

though this limit is less reliable than the laboratory one (4), and probably four neutrino species can still be tolerated [15]. In view of (4), the additional neutrino species, if exist, must be a sterile neutrino  $\nu_s$ .

Are neutrinos Dirac or Majorana particles? The only practical way of answering this question, known at the moment, is to look for the neutrinoless double beta decay

$$A(Z, N) \rightarrow A(Z \pm 2, N \mp 2) + 2e^\mp. \quad (6)$$

This process can only occur if neutrinos are Majorana particles. If  $2\beta 0\nu$  decay is mediated by the standard weak interactions, the amplitude of the process is proportional to the effective neutrino mass

$$A(2\beta 0\nu) \propto \sum_i U_{ei}^2 m_i \equiv \langle m_{\nu_e} \rangle_{eff}, \quad (7)$$

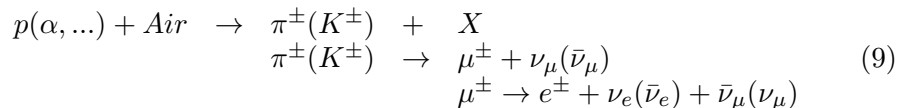
where  $U_{ai}$  is the lepton mixing matrix. Neutrinoless double beta decay was searched for experimentally but up to now have not been discovered. The experiments allowed to put upper bounds on the effective Majorana neutrino mass, the best limit coming from the Heidelberg – Moscow experiment on  $2\beta$  decay of  $^{76}\text{Ge}$  [16]:

$$\langle m_{\nu_e} \rangle_{eff} < 0.2 - 0.6 \text{ eV}, \quad (8)$$

depending on the value of the nuclear matrix element which is not precisely known. If the  $2\beta 0\nu$  decay is discovered, it will be possible to infer the value of the effective Majorana neutrino mass  $\langle m_{\nu_e} \rangle_{eff}$ . As follows from (7), this would give the lower limit on the mass of the heaviest neutrino. For a recent review of  $2\beta$  decay experiments, see [17].

### 3. Atmospheric neutrinos

are electron and muon neutrinos and their antineutrinos which are produced in the hadronic showers induced by primary cosmic rays in the earth's atmosphere. The main mechanism of production of the atmospheric neutrinos is given by the following chain of reactions:



Atmospheric neutrinos can be observed directly in large mass underground detectors predominantly by means of their charged current (CC) interactions:

$$\begin{aligned}\nu_e(\bar{\nu}_e) + A &\rightarrow e^-(e^+) + X, \\ \nu_\mu(\bar{\nu}_\mu) + A &\rightarrow \mu^-(\mu^+) + X.\end{aligned}\tag{10}$$

Calculations of the atmospheric neutrino fluxes predict the  $\nu_\mu/\nu_e$  ratio that depends on neutrino energy and the zenith angle of neutrino trajectory, approaching 2 for low energy neutrinos and horizontal trajectories but exceeding this value for higher energy neutrinos and for trajectories close to vertical. The overall uncertainty of the calculated atmospheric neutrino fluxes is rather large, and the total fluxes calculated by different authors differ by as much as 20 – 30%. At the same time, the ratio of the muon to electron neutrino fluxes is fairly insensitive to this uncertainty, and different calculations yield the ratios of muon-like to electron-like contained events which agree to about 5%. This ratio has been measured in a number of experiments, and the Kamiokande and IMB Collaborations reported smaller than expected ratio in their contained events, with the double ratio  $R(\mu/e) \equiv [(\nu_\mu + \bar{\nu}_\mu)/(\nu_e + \bar{\nu}_e)]_{data}/[(\nu_\mu + \bar{\nu}_\mu)/(\nu_e + \bar{\nu}_e)]_{MC} \simeq 0.6$  where MC stands for Monte Carlo simulations. The discrepancy between the observed and predicted atmospheric neutrino fluxes was called the atmospheric neutrino anomaly. The existence of this anomaly was subsequently confirmed by Soudan 2, MACRO and Super-Kamiokande experiments. Most remarkably, the Super-Kamiokande (SK) Collaboration obtained a very convincing evidence for the up-down asymmetry and zenith-angle dependent deficiency of the flux of muon neutrinos, which has been interpreted as an evidence for neutrino oscillations. We shall now discuss the SK data and their interpretation.

The SK detector is a 50 kt water Cherenkov detector (22.5 kt fiducial volume) which is overseen by more than 13,000 photomultiplier tubes. The charged leptons born in the CC interactions of neutrinos produce the rings of the Cherenkov light in the detector which are observed by the phototubes. Muons can be distinguished from electrons since their Cherenkov rings are sharp whereas those produced by electrons are diffuse. The SK Collaboration subdivided their atmospheric neutrino events into several groups, depending on the energy of the charged leptons produced. Fully contained (FC) events are those for which the neutrino interaction vertex is located inside the detector and all final state particles do not get out of it. FC events are further subdivided into sub-GeV (visible energy < 1.33 GeV) and multi-GeV (visible energy > 1.33 GeV) events. Partially contained (PC) events are those for which the produced muon exits the inner detector volume (only muons are penetrating enough). The average energy

of a neutrino producing a PC event in SK is  $\sim 15$  GeV. Muon neutrinos can also be detected indirectly by observing the muons that they have produced in the material surrounding the detector. To reduce the background from atmospheric muons, only upward-going neutrino-induced muons are usually considered. A rough estimate of the energy spectrum of the upward-going muons has been obtained dividing them in two categories, passing (or through-going) and stopping muons. The latter, which stop inside the detector, correspond to the average parent neutrino energy  $\sim 10$  GeV, whereas for the through-going muons the average neutrino energy is  $\sim 100$  GeV.

The measurements of the double ratio  $R(\mu/e)$  for contained events at SK (1144 live days) give [18, 19]

$$\begin{aligned} R &= 0.652 \pm 0.019 (stat.) \pm 0.051 (syst.) \quad (\text{sub-GeV}), \\ R &= 0.668 \pm 0.034 (stat.) \pm 0.079 (syst.) \quad (\text{multi-GeV}). \end{aligned} \quad (11)$$

The value of  $R$  for sub-GeV events is different from unity (to which it should be equal in no-oscillation case) by more than  $6\sigma$ .

We shall now discuss the zenith angle distributions of the atmospheric neutrino events. It should be remembered that the zenith angle distributions of charged leptons which are experimentally measured do not coincide with those of their parent neutrinos: for multi-GeV neutrinos the average angle between the momenta of neutrinos and charged leptons is about  $17^\circ$ , whereas for sub-GeV neutrinos it is close to  $60^\circ$ . This is properly taken into account in MC simulations. For PC events and upward going muons the correlation between the directions of momenta of muons and parent neutrinos is much better. The distances  $L$  traveled by neutrinos before they reach the detector vary in a wide range: for vertically downward going neutrinos (neutrino zenith angle  $\Theta_\nu = 0$ )  $L \sim 15$  km; for horizontal neutrino trajectories ( $\Theta_\nu = 90^\circ$ )  $L \sim 500$  km; the vertically up-going neutrinos ( $\Theta_\nu = 180^\circ$ ) cross the earth along its diameter and for them  $L \sim 13,000$  km.

In fig. 1 the zenith angle distributions of the SK e-like and  $\mu$ -like events are shown separately for sub-GeV and multi-GeV contained events. One can see that for e-like events, the measured zenith angle distributions agree very well with the MC predictions (shown by bars), both in the sub-GeV and multi-GeV samples, while for  $\mu$ -like events both samples show zenith-angle dependent deficiency of event numbers compared to expectations. The deficit of muon neutrinos is stronger for upward going neutrinos which have larger pathlengths. In the multi-GeV sample, there is practically no deficit of events caused by muon neutrinos coming from the upper hemisphere ( $\cos \Theta > 0$ ), whereas in the sub-GeV sample, all  $\mu$ -like events exhibit a deficit which decreases with  $\cos \Theta$ . This pattern is perfectly consistent with oscillations  $\nu_\mu \leftrightarrow \nu_\tau$  or  $\nu_\mu \leftrightarrow \nu_s$  where  $\nu_s$  is a sterile neutrino. Muon neutrinos responsible for the multi-GeV sample are depleted by the oscillations

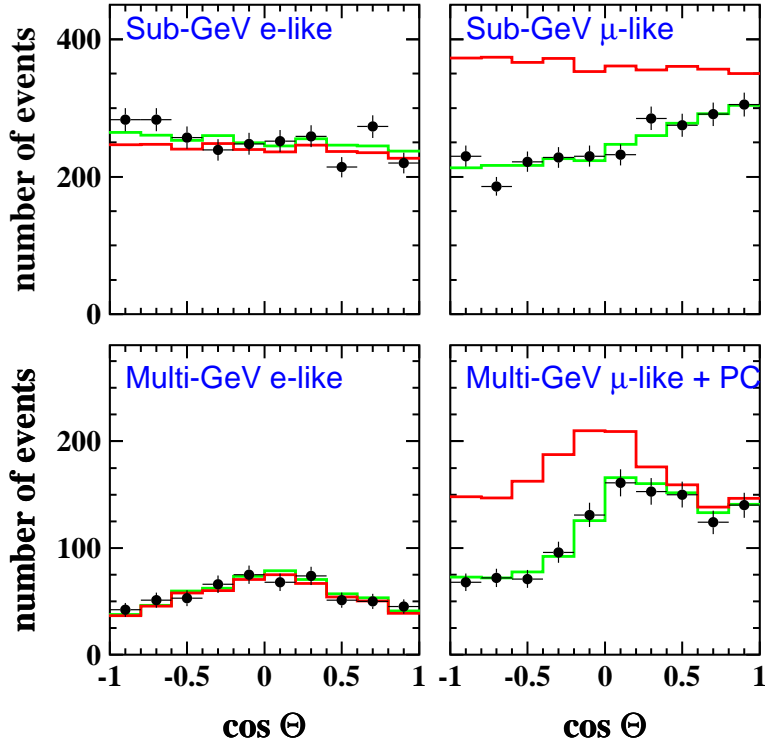


Figure 1. Zenith angle distributions for sub-GeV and multi-GeV e-like and  $\mu$ -like events at SK (1144 live days). The dark-hatched lines show the (no-oscillations) Monte Carlo predictions; light-hatched lines show the predictions for  $\nu_\mu \leftrightarrow \nu_\tau$  oscillations with the best-fit parameters  $\Delta m^2 = 3.2 \times 10^{-3} \text{ eV}^2$ ,  $\sin^2 2\theta = 1.0$  [18].

when their pathlength is large enough; the depletion becomes less pronounced as the pathlength decreases ( $\cos \Theta$  increases); for neutrinos coming from the upper hemisphere, the pathlengths are too short and there are practically no oscillations. Neutrinos responsible for the sub-GeV  $\mu$ -like events have smaller energies, and so their oscillation lengths are smaller; therefore even neutrinos coming from the upper hemisphere experience sizeable depletion due to the oscillations. For up-going sub-GeV neutrinos the oscillation length is much smaller than the pathlength and they experience averaged oscillations. The solid line in fig. 1 obtained with the  $\nu_\mu \leftrightarrow \nu_\tau$  oscillation parameters in the 2-flavour scheme  $\Delta m^2 = 3.2 \times 10^{-3} \text{ eV}^2$ ,  $\sin^2 2\theta = 1.0$  gives an excellent fit of the data.

An informative parameter characterizing the distortion of the zenith angle distribution is the up-down event ratio  $U/D$ , where up corresponds to the events with  $\cos \Theta < -0.2$  and down to those with  $\cos \Theta > 0.2$ . The flux of atmospheric neutrinos is expected to be nearly up-down symmetric for neutrino energies  $E \gtrsim 1 \text{ GeV}$ , with minor deviations coming from ge-

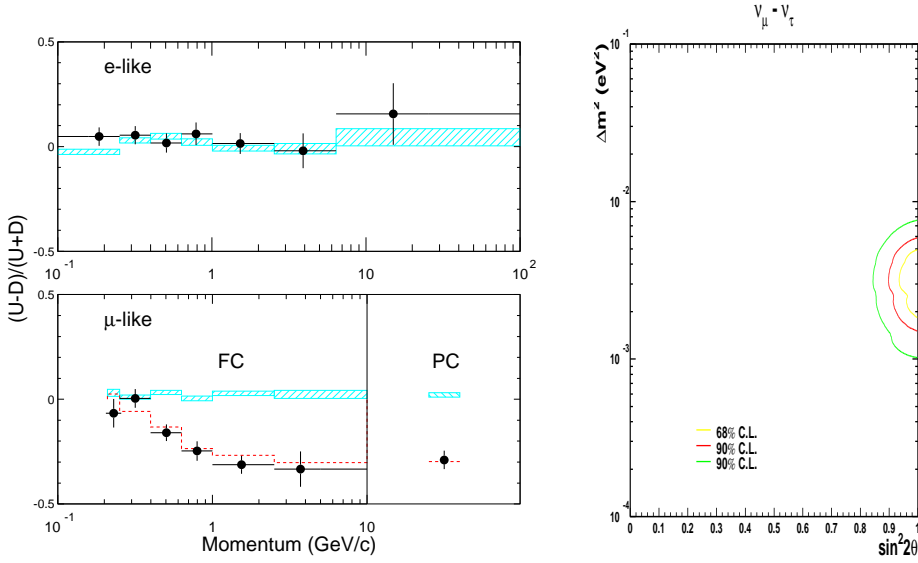


Figure 2. Left panel: up-down asymmetry vs event momentum for single ring e-like and  $\mu$ -like events in SK (1144 live days). Hatched bricks – no oscillations, dashed line corresponds to  $\nu_\mu \leftrightarrow \nu_\tau$  oscillations with  $\Delta m^2 = 3.2 \times 10^{-3} \text{ eV}^2$ ,  $\sin^2 2\theta = 1$ . Right panel: SK allowed regions of oscillations parameters for  $\nu_\mu \leftrightarrow \nu_\tau$  channel in 2-flavour scheme (FC + PC events) [18].

omagnetic effects which are well understood and can be accurately taken into account. In particular, at the geographical location of the SK detector small upward asymmetry is expected, i.e.  $U/D$  should be slightly bigger than 1. Any significant deviation of the up-down asymmetry of neutrino induced events from the asymmetry due to the geomagnetic effects is an indication of neutrino oscillations or some other new neutrino physics. The  $U/D$  ratio measured for the SK multi-GeV  $\mu$ -like events is [18, 19]

$$U/D = 0.54 \pm 0.04 (\text{stat.}) \pm 0.01 (\text{syst.}), \quad (12)$$

i.e. is below unity by about  $9\sigma$ ! The dependence of the asymmetries for e-like FC and  $\mu$ -like FC+PC events on the event momentum is shown in fig. 2 (left panel). One can see that for e-like events the asymmetry  $A \equiv (U - D)/(U + D) \simeq 0$  for all momenta. At the same time, for  $\mu$ -like events the asymmetry is close to zero at low momenta and decreases with momentum. This is easily understood in terms of the  $\nu_\mu$  oscillations. For very small momenta, the oscillation length is small and both up-going and down-going neutrino fluxes are depleted by oscillations to about the same extent; in addition, loose correlation between the directions of the momenta of the charged lepton and of its parent neutrino tends to smear out the asymmetry at low energies. With increasing momentum the oscillation length increases, and

the pathlength of down-going neutrinos becomes too small for oscillations to develop.

The SK data show evidence for neutrino oscillations not only in their FC and PC  $\mu$ -like events: upward stopping and upward through-going events also demonstrate zenith angle dependent deficiency of muon neutrinos consistent with neutrino oscillations, although the statistics for up-going muons is lower than that for contained events. The combined analysis of the SK FC, PC and upward muon event data yields the best-fit values  $\Delta m^2 = 3.2 \times 10^{-3} \text{ eV}^2$  and  $\sin^2 2\theta = 1.0$ , with the very high quality of the fit:  $\chi^2/d.o.f. = 135.4/152$ . This value has to be compared with that of the no-oscillation hypothesis:  $\chi^2/d.o.f. = 316.2/154$ , which is a very poor fit.

Are neutrino oscillations that are responsible for the depletion of the  $\nu_\mu$  flux  $\nu_\mu \leftrightarrow \nu_\tau$  or  $\nu_\mu \leftrightarrow \nu_s$ ? For contained events, the oscillation probabilities in these two channels are nearly the same and the data can be fitted equally well in both cases, with very similar allowed ranges of the oscillation parameters. However, for higher energy PC and upward going events there are important differences between these two cases. In the 2-flavour scheme,  $\nu_\mu \leftrightarrow \nu_\tau$  oscillations are not affected by matter because the interactions of  $\nu_\mu$  and  $\nu_\tau$  with matter are identical. However, sterile neutrinos do not interact with matter at all, and therefore the  $\nu_\mu \leftrightarrow \nu_s$  oscillations are affected by the matter-induced potential  $V_\mu - V_s = V_\mu$ . At low energies, the kinetic energy difference  $\Delta m^2/2E$  dominates over  $V_\mu$ , and the earth's matter effects are unimportant. They become important at higher energies, when  $\Delta m^2/2E \sim V_\mu$ ; at very high energies, when  $\Delta m^2/2E \ll V_\mu$ , matter strongly suppresses neutrino oscillations both in  $\nu_\mu \leftrightarrow \nu_s$  and  $\bar{\nu}_\mu \leftrightarrow \bar{\nu}_s$  channels. Therefore the oscillations of high energy neutrinos traveling significant distances in the earth should be strongly suppressed in this case. Such a suppression was searched for in PC and upward through-going event samples, but has not been observed. This fact together with the analysis of the neutral current enriched multi-ring events allowed the SK Collaboration to exclude pure  $\nu_\mu \rightarrow \nu_s$  oscillations at the 99% c.l. [18, 19, 20]. The oscillations into sterile neutrinos are, however, allowed in the 4-neutrino framework, with the weight that can be as large as about 50% [21]<sup>1</sup>.

Can  $\nu_\mu \leftrightarrow \nu_e$  oscillations be responsible for the observed anomalies in the atmospheric neutrino data? The answer is no, at least not as the dominant channel. Explaining the data requires oscillations with large mixing equal or close to the maximal one;  $\nu_\mu \leftrightarrow \nu_e$  oscillations would then certainly lead to a significant distortion of the zenith angle distributions of the e-like contained events, contrary to observations. In addition, for  $\Delta m^2$  in the range  $\sim 10^{-3} \text{ eV}^2$  which is required by the atmospheric neutrino data,  $\nu_\mu \leftrightarrow$

<sup>1</sup>It should be noted, however, that the analysis of [21] does not include the SK neutral current enriched multi-ring event sample.

$\nu_e$  oscillations are severely restricted by the CHOOZ reactor antineutrino experiment [22], which excludes these oscillations as the main channel of the atmospheric neutrino oscillations.

However,  $\nu_\mu \leftrightarrow \nu_e$  and  $\nu_e \leftrightarrow \nu_\tau$  can be present as subdominant channels of the oscillations of atmospheric neutrinos. This may lead to interesting matter effects on oscillations of neutrinos crossing the earth on their way to the detector. Matter can strongly affect  $\nu_e \leftrightarrow \nu_{\mu,\tau}$  and  $\bar{\nu}_e \leftrightarrow \bar{\nu}_{\mu,\tau}$  oscillations leading to an enhancement of the oscillation probabilities for neutrinos and suppression for antineutrinos or vice versa, depending on the sign of the corresponding mass squared difference.

Since three neutrino flavours are known to exist, oscillations of atmospheric neutrinos should in general be considered in the full 3-flavour framework (assuming that no sterile neutrinos take part in these oscillations). Three flavour analyses [18, 19, 23, 24] only slightly modify the 2-flavour results, which is a consequence of the smallness of the leptonic mixing parameter  $U_{e3}$

Are the standard neutrino oscillations the sole possible explanation of the observed atmospheric neutrino anomalies? In principle, other explanations are possible. Those include exotic types of neutrino oscillations – matter-induced oscillations due to flavour-changing interactions of neutrinos with medium, oscillations due to small violations of the Lorentz or CPT invariance or of the gravitational equivalence principle, and also neutrino decay. Exotic oscillations lead to periodic variations of the  $\nu_\mu$  survival probability with the oscillation lengths  $l_{osc} \propto E^{-n}$  where  $n = 0$  in the case of flavour-changing neutrino interactions or violation of CPT invariance, and  $n = 1$  for oscillations due to the violations of the Lorentz invariance or equivalence principle. This has to be contrasted with  $n = -1$  in the case of the standard neutrino oscillations. The energy dependence of the oscillation length can be tested in the atmospheric neutrino experiments as the energies of detected neutrinos span more than 3 orders of magnitude. The first analysis was performed in [25], and the authors found that the fit of the atmospheric neutrino data assuming oscillations with  $l_{osc} \propto E^{-n}$  gives  $n = -0.9 \pm 0.4$  at 90% c.l.. The SK Collaboration has recently performed a similar analysis of their full 1144 days sample of events, which gave  $n = -1.06 \pm 0.14$  [18, 19]. These results clearly favour the standard oscillations over the exotic ones. In contrast to this, the neutrino decay mechanism fits the SK data quite well, the quality of the fit being as good as the one for the standard neutrino oscillations [26]. The reason for this is that the oscillations and decay lead to very similar averaged survival probabilities for  $\nu_\mu$ . One could discriminate between the two solutions in the experiments like the recently proposed MONOLITH [27]. The MONOLITH detector will have a much better  $L/E$  resolution than that of the

SK, and therefore will be able to clearly detect the full first oscillation swing of the  $\nu_\mu$  survival probability (i.e. not only disappearance but also reappearance of  $\nu_\mu$ ) in the case of the neutrino oscillation solution of the atmospheric neutrino anomaly.

#### 4. The solar neutrino problem

The first experiment in which the solar neutrinos have been observed was the Homestake experiment of Davis and his collaborators. It is based on the reaction



The energy threshold of reaction (13) is 0.814 MeV, so only the  ${}^8\text{B}$  and  ${}^7\text{Be}$  and  $pp$  neutrinos are detected in the Homestake experiment (see fig. 3), the largest contribution coming from the  ${}^8\text{B}$  neutrinos. The two gallium solar neutrino experiments, SAGE and Gallex, employ the reaction



The energy threshold of this reaction is 0.233 MeV, and so the gallium experiments can also detect the lowest energy  $pp$  neutrinos. The next two experiments – Kamiokande and its up-scaled version Super-Kamiokande – are the water Cherenkov detectors and use the neutrino-electron scattering reaction



to detect solar neutrinos. This reaction has zero physical threshold, but one has to introduce energy cuts to suppress the background. In the Kamiokande experiment solar neutrinos with the energies  $E > 7.5$  MeV were detected, whereas the threshold used by Super-Kamiokande (SK) in their analysis is at present 5.5 MeV. With these energy cuts, the Kamiokande and SK detection rates are only sensitive to the  ${}^8\text{B}$  component of the solar neutrino flux (the highest-energy  $hep$  neutrinos give a negligible contribution to the total detection rates as their flux is very low).

In all five solar neutrino experiments (Homestake, Gallex, SAGE, Kamiokande and SK) fewer neutrinos than expected were detected, the degree of deficiency being different in the experiments of different types (see table I). This has been called the solar neutrino problem.

The solar neutrino problem is not just the problem of the deficit of the observed neutrino flux: results of different experiments seem to be inconsistent with each other. In the absence of new neutrino physics, the energy spectra of the various components of the solar neutrino flux are given by the standard nuclear physics and well known, and only the total fluxes of these components may be different from those predicted by the standard solar

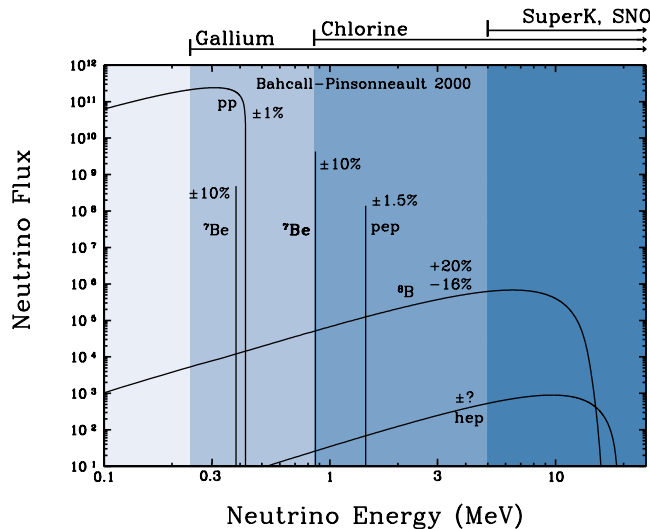


Figure 3. Solar neutrino spectrum and estimated theoretical errors of fluxes. The thresholds of solar neutrino experiments are indicated above the figure. From [28].

TABLE 1. Detection rates in five solar neutrino experiments. Units are SNU (1 SNU =  $10^{-36}$  captures per target atom per second) for all the experiments except Kamiokande and SK, for which they are  $10^6 \text{ cm}^{-2} \text{ s}^{-1}$ . From [30].

Experiment	Data	Theory (BP98)	Data/Theory
Homestake	$2.56 \pm 0.16 \pm 0.14$	$7.7 \pm_{1.0}^{1.2}$	$0.33 \pm 0.027$
Kamiokande	$2.80 \pm 0.19 \pm 0.33$	$5.15 \pm_{0.7}^{1.0}$	$0.54 \pm 0.07$
SAGE	$75.4 \begin{smallmatrix} +7.0 & +3.5 \\ -6.8 & -3.0 \end{smallmatrix}$	$129 \begin{smallmatrix} +8 \\ -6 \end{smallmatrix}$	$0.58 \pm 0.06$
Galex+GNO	$74.1 \begin{smallmatrix} +6.7 \\ -6.8 \end{smallmatrix}$	$129 \begin{smallmatrix} +8 \\ -6 \end{smallmatrix}$	$0.57 \pm 0.06$
Super-Kamiokande	$2.40 \pm 0.03 \begin{smallmatrix} +0.08 \\ -0.07 \end{smallmatrix}$	$5.15 \pm_{0.7}^{1.0}$	$0.465 \pm 0.016$

models. The fluxes inferred from different experiments are not consistent with each other, and in fact the best fit value of the the  ${}^7\text{Be}$  neutrino flux is negative! One is then led to conclude that neutrinos are not standard.

There are several possible particle-physics solutions of the solar neutrino problem, the most natural one being neutrino oscillations. The neutrino oscillation solution has become even more plausible after the strong evidence for atmospheric neutrino oscillations was reported by the SK Collaboration. Neutrino oscillations can convert a fraction of solar  $\nu_e$  into  $\nu_\mu$  or  $\nu_\tau$  (or their combination). Since the energy of solar neutrinos is smaller than the masses of muons and taus, these  $\nu_\mu$  or  $\nu_\tau$  cannot be detected in the CC reactions of the type (13) or (14) and therefore are invisible in the chlorine and gallium experiments. They can scatter on electrons through the

neutral current (NC) interactions and therefore should contribute to the detection rates in water Cherenkov detectors. However, the cross section of the NC channel of reaction (15) is about a factor of 6 smaller than that of the CC channel, and so the deficit of the neutrino flux observed in the Kamiokande and SK experiments can be explained. The probabilities of neutrino oscillations depend on neutrino energy, and the distortion of the energy spectrum of the experimentally detected solar neutrinos, which is necessary to reconcile the data of different experiments, is readily obtained.

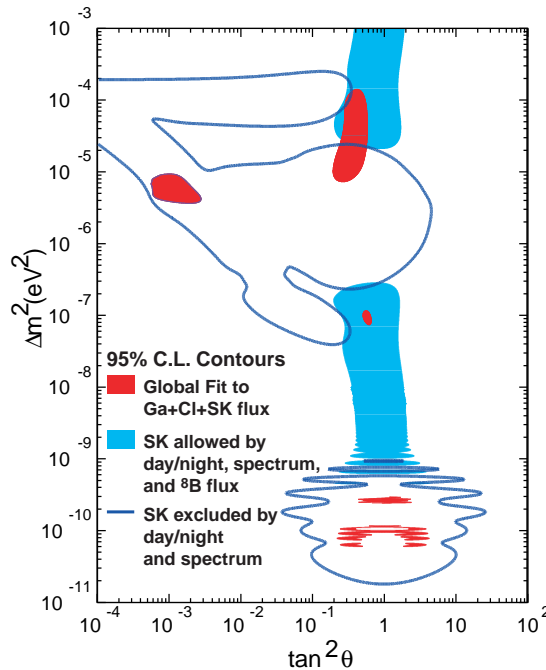


*Figure 4.* Solar neutrino parameter space: the dark areas show the global flux fit solutions. The interiors of the dark lines indicate the SK excluded regions; the light shaded areas indicate the SK allowed regions [31].

The oscillations of solar neutrinos inside the sun can be strongly enhanced due to the MSW effect [30] and the solar data can be fitted even with a very small vacuum mixing angle. Solar matter can also influence neutrino oscillations if the vacuum mixing angle is not small. The allowed values of the neutrino oscillation parameters  $\tan^2\theta$  and  $\Delta m^2$  which fit the detection rates in the chlorine, gallium and water Cherenkov experiments in the 2-flavour scheme are shown in fig. 4 for oscillations of  $\nu_e$  into active neutrinos (dark shaded areas). In the case of the matter enhanced oscillations, there are three allowed ranges of the parameters corresponding to the

small mixing angle (SMA), large mixing angle (LMA) and low  $\Delta m^2$  (LOW) MSW solutions. There is also the vacuum oscillation (VO) solution corresponding to very small values of  $\Delta m^2$ , for which the neutrino oscillation length for typical solar neutrino energies ( $\sim$  a few MeV) is comparable to the distance between the sun and the earth. This solution is also known as “just so” oscillation solution. The detection rates in the five solar neutrino experiments can also be explained by  $\nu_e \rightarrow \nu_s$  oscillations, for which there is only the SMA solution with the allowed region of parameters similar to that for oscillations into active neutrinos [31, 32].

The use of the variable  $\tan^2 \theta$  instead of the usual  $\sin^2 2\theta$  in fig. 4 is worth a comment. The probability of 2-flavour neutrino oscillations in vacuum is invariant under the substitutions  $\theta \rightarrow \pi/2 - \theta$  or  $\Delta m^2 \rightarrow -\Delta m^2$ , but the oscillation probability in matter is not. It is, however, invariant under the combined action of these substitutions. To cover the full parameter space it is sufficient to assume  $0 \leq \theta \leq \pi/4$  and allow for both signs of  $\Delta m^2$ , or to assume that  $\Delta m^2$  is always positive (which can always be achieved by renaming the mass eigenstates  $\nu_1 \leftrightarrow \nu_2$ ) and let  $\theta$  be in the full domain  $[0, \pi/2]$ . Usually, the first approach was adopted; however, the solutions of the solar neutrino problem in the region  $\Delta m^2 < 0$  have not been studied (except in the 3-neutrino [33] and 4-neutrino [34] frameworks). This was motivated by the fact that there is no MSW enhancement for neutrinos in this region of parameters. However, in [35] it has been emphasized that if one allows for large enough confidence levels, or treats the solar  ${}^8\text{B}$  neutrino flux as a free parameter, or leaves the Homestake result out, solutions in this “dark side” of the parameter space exist, provided that the mixing angle is close to the maximal one. It is convenient to assume  $\Delta m^2 > 0$  and plot the allowed regions of the parameter space in the plane  $(\tan^2 \theta, \Delta m^2)$  with  $0 \leq \theta \leq \pi/2$ ; in the conventional approach one would need two separate plots for  $\Delta m^2 > 0$  and  $\Delta m^2 < 0$ .

Solar neutrinos detected during night travel some distance inside the earth on their way to the detector, and their oscillations can be affected by the matter of the earth. In particular, a fraction of  $\nu_\mu$  or  $\nu_\tau$  produced as a result of the solar  $\nu_e$  oscillations can be reconverted into  $\nu_e$  by oscillations enhanced by the matter of the earth. The day/night difference due to the earth “regeneration” effect (and in general the zenith angle dependence of the neutrino signal) can in principle be observed in real-time experiments, such as SK. The day/night effect is expected to be appreciable in the case of the LMA solution, but very small in the case of the SMA solution. For the LOW solution, the day/night effect is expected to be quite sizeable in the low-energy part of the solar neutrino spectrum (in particular, for  ${}^7\text{Be}$  neutrinos), but small for the high-energy part detected by SK. There is no day/night effect in the case of the VO solution.

The zenith angle dependence of the solar neutrino signal measured by the SK is shown in fig. 5. The value of day/night asymmetry measured in

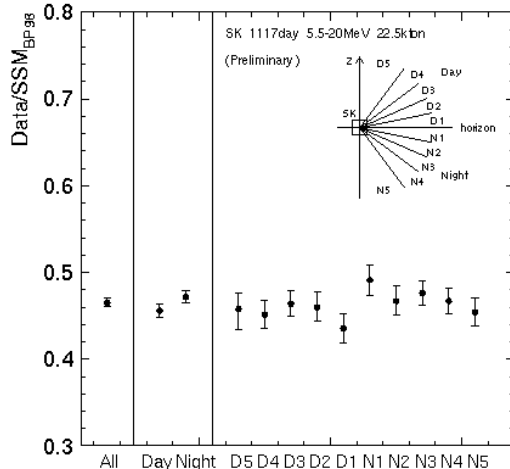


Figure 5. Zenith angle dependence of the solar neutrino flux measured by the Super-Kamiokande experiment [31].

the SK experiment is [31]

$$\frac{D - N}{(D + N)/2} = -0.034 \pm 0.022 (stat.)_{-0.012}^{+0.013} (syst.), \quad (16)$$

i.e. shows an excess of the night-time flux at about  $1.3\sigma$ . This excess, however, is not statistically significant. The smallness of the SK day/night asymmetry results in the exclusion of the lower- $\Delta m^2$  part of the LMA allowed region (see fig. 4). This is a good news for future very long baseline accelerator experiments as it improves the prospects of observation of CP violation in neutrino oscillations. The zenith angle event dependence measured by the SK shows a rather flat distribution of the excess of events over different night-time zenith angle bins. This is rather typical for the LMA and LOW solutions (although for LOW solution one can expect some excess of events in the second night bin  $N2$  [36]), whereas for the SMA solution one normally expects the excess (or deficiency) to be concentrated in the vertical upward bin with zenith angles  $\theta$  in the range  $-1 < \cos \theta < -0.8$ .

Neutrino oscillations should result in certain distortions of the spectrum of the detected solar neutrinos, which can be studied by measuring the recoil electron spectrum in the reaction (15). This spectrum has been measured in the SK experiment, and the results are shown in fig. (6). In the absence of the neutrino spectrum distortion, the ratio measured/expected

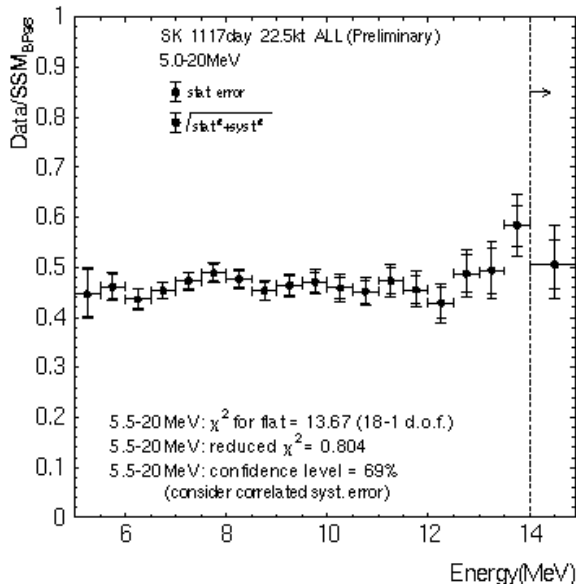


Figure 6. Recoil electron energy spectrum in the Super-Kamiokande experiment normalized to the standard solar model prediction. From [31].

electron spectrum presented in this figure should be a horizontal line. The measured relative spectrum is rather flat; in particular, the excess of high-energy events seen in the earlier SK data has essentially disappeared. This allowed SK to put an upper limit on the flux of the *hep* neutrinos:  $f_{hep} < 13.2 f_{hep}(\text{BP98})$ , with the best fit value  $f_{hep} = (5.4 \pm 4.5) f_{hep}(\text{BP98})$ , where BP98 stands for the Bahcall-Pinsonneault 98 standard solar model.

The flatness of the SK relative spectrum disfavors the VO solution and the larger- $\sin^2 2\theta$  part of the SMA parameter space; on the other hand the small- $\sin^2 2\theta$  part of the SMA parameter space is disfavoured since it predicts a positive day-night asymmetry while the asymmetry measured by SK is negative (at  $1.3\sigma$  level). This allowed the SK Collaboration to conclude that at present the VO and SMA solutions are disfavoured at 95% c.l., while the LMA and LOW solutions are favoured (see fig. 4). Oscillations into sterile neutrinos are also disfavoured at 95% c.l..

While this result is certainly interesting and shows the directions in which the solar neutrino data seem to lead us, one should clearly understand that in fact the VO and SMA solutions are *not* yet excluded. The solar neutrino data are not fully settled yet, and caution is advised when drawing conclusions. It is worth remembering that just a few years ago the LOW solution, which is now a perfectly respectable one, was disfavoured, and shortly before that it just did not exist. Obviously, more data are needed

to clear the situation up.

Fortunately, several new experiments which can potentially resolve the problem are now under way or will be soon put into operation. The SNO (Sudbury Neutrino Observatory) experiment started taking data last year, and its first results were reported at the Neutrino 2000 Conference [37]. The SNO detector consists of 1000 tons of heavy water, and is capable of detecting solar neutrinos in three different channels:

$$\nu_e + d \rightarrow p + p + e^- \quad (\text{CC}), \quad E_{min} = 1.44 \text{ MeV}, \quad (17)$$

$$\nu_a + d \rightarrow p + n + \nu_a \quad (\text{NC}), \quad E_{min} = 2.23 \text{ MeV}, \quad (18)$$

and  $\nu_a e$  scattering process (15) which can proceed through both CC and NC channels. The CC reaction (17) is very well suited for measuring the solar neutrino spectrum: unlike in the case of  $\nu_a e$  scattering (15) in which the energy of incoming neutrino is shared between two light particles in the final state, the final state of the reaction (17) contains only one light particle – electron, and a heavy  $2p$  system whose kinetic energy is relatively small. Therefore the electron energy is strongly correlated with the energy of the incoming neutrino. The CC electron spectrum measured by SNO (fig. 7) confirms the flat spectrum measured by SK. The absolute value of the solar neutrino flux measured in the CC reaction has not been given since the analysis of the data is still under way.

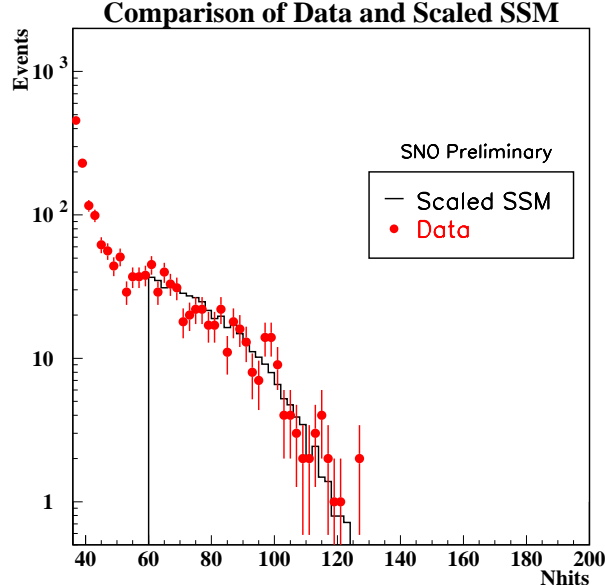


Figure 7. CC electron spectrum (distribution of events vs number of PMT hits). The line is a scaled standard solar model prediction. The scaling factor is not specified. From [37].

The cross section of the NC reaction (18) is the same for neutrinos of all three flavours, and therefore oscillations between  $\nu_e$  and  $\nu_\mu$  or  $\nu_\tau$  would not change the NC detection rate in the SNO experiment. On the other hand, these oscillations would deplete the solar  $\nu_e$  flux, reducing the CC event rate. Therefore the CC/NC ratio is a sensitive probe of neutrino flavour oscillations. If solar  $\nu_e$  oscillate into electroweak singlet (sterile) neutrinos, both CC and NC event rates will be suppressed.

The Borexino experiment is scheduled to start taking data in 2002. It will detect solar neutrinos through the  $\nu_a e$  scattering with a very low energy threshold, and will be able to detect the  ${}^7\text{Be}$  neutrino line. Different solutions of the solar neutrino problem predict different degree of suppression of  ${}^7\text{Be}$  neutrinos, and their detection could help discriminate between these solutions. Observation of the  ${}^7\text{Be}$  neutrino line would be especially important in the case of the VO solution. Due to the eccentricity of the earth's orbit the distance between the sun and the earth varies by about 3.5% during the year, and this should lead to varying oscillation phase (and therefore varying solar neutrino signal) in the case of vacuum neutrino oscillations. This seasonal variation can in principle be separated from the trivial 7% variation due to the  $1/L^2$  law which is not related to neutrino oscillations<sup>2</sup>. Since the oscillation phase depends on neutrino energy, integration over significant energy intervals may make it difficult to observe the seasonal variations of the solar neutrino flux due to VO. The  ${}^7\text{Be}$  neutrinos are monochromatic, which should facilitate the observation of the seasonal variations at Borexino.

Borexino will also be capable of confirming or refuting the LOW solution: a strong day/night effect predicted for  ${}^7\text{Be}$  neutrinos by this solution should be clearly detectable at Borexino [38]. On the other hand, the LMA solution will be tested by the KamLAND experiment, which will start taking data in 2001. Although it will be a reactor neutrino experiment, its very long baseline will enable it to probe very small values of  $\Delta m^2$ , relevant for the LMA solution (see the next section). One can hope that the combined data of the currently operating and forthcoming experiments will allow to finally resolve the solar neutrino problem.

## 5. Reactor and accelerator neutrino experiments

In reactor neutrino experiments oscillations of electron antineutrinos into another neutrino species are searched for by studying possible depletion of the  $\bar{\nu}_e$  flux beyond the usual geometrical one. These are the disappearance experiments, because the energies of the reactor  $\bar{\nu}_e$ 's ( $\langle E \rangle \simeq 3 \text{ MeV}$ ) are too

<sup>2</sup>The seasonal dependence of the SK detection rate is in a good agreement with the  $1/L^2$  law, with  $\chi^2/d.o.f. = 4.1/7$  (goodness of fit 76%).

small to allow the detection of muon or tauon antineutrinos in CC experiments. Small  $\bar{\nu}_e$  energy makes the reactor neutrino experiments sensitive to oscillations with rather small values of  $\Delta m^2$ .

Up to now, no evidence for neutrino oscillations has been found in the reactor neutrino experiments, which allowed to exclude certain regions in the neutrino parameter space. The best constraints were obtained by the CHOOZ experiment in France [22]. For the values of  $\Delta m_{31}^2 \equiv \Delta m_{atm}^2$  in the SK allowed region  $(1.5 - 5) \times 10^{-3} \text{ eV}^2$ , the CHOOZ results give the following constraint on the element  $U_{e3}$  of the lepton mixing matrix:  $|U_{e3}|^2(1 - |U_{e3}|^2) < 0.055 - 0.015$  at 90% c.l., i.e.  $|U_{e3}|$  is either small or close to unity. The latter possibility is excluded by solar and atmospheric neutrino observations, and one finally obtains <sup>3</sup>

$$\sin^2 \theta_{13} \equiv |U_{e3}|^2 \leq (0.06 - 0.018) \quad \text{for} \quad \Delta m_{31}^2 = (1.5 - 5) \times 10^{-3} \text{ eV}^2. \quad (19)$$

This is the most stringent constraint on  $|U_{e3}|$  to date.

Presently, a long baseline reactor experiment KamLAND is under construction in Japan. This will be a large liquid scintillator detector experiment using the former Kamiokande site. KamLAND will detect electron antineutrinos coming from several Japanese and Korean power reactors at an average distance of about 180 km. KamLAND is scheduled to start taking data in 2001 and will be sensitive to values of  $\Delta m^2$  as low as  $4 \times 10^{-6} \text{ eV}^2$ , i.e. in the range relevant for the solar neutrino oscillations! It is expected to be able to probe the LMA solution of the solar neutrino problem (see fig. 8). It may also be able to directly detect solar  $^8\text{B}$  and  $^7\text{Be}$  neutrinos after its liquid scintillator has been purified to ultra high purity level by recirculating through purification.

There have been a number of accelerator experiments looking for neutrino oscillations. In all but one no evidence for oscillations was found and constraints on oscillation parameters were obtained. The LSND Collaboration have obtained an evidence for  $\bar{\nu}_\mu \rightarrow \bar{\nu}_e$  and  $\nu_\mu \rightarrow \nu_e$  oscillations [39]. The LSND result is the only indication for neutrino oscillations that is a signal and not a deficiency. The KARMEN experiment [40] is looking for neutrino oscillations in  $\bar{\nu}_\mu \rightarrow \bar{\nu}_e$  channel. No evidence for oscillations has been obtained, and part of the LSND allowed region has been excluded. In fig. 9 the results from LSND and KARMEN experiments are shown along with the relevant constraints from the BNL E776, CCFR, CHOOZ and Bugey experiments. One can see that the only domain of the

<sup>3</sup>We use the parametrization of the  $3 \times 3$  lepton mixing matrix which coincides with the standard parametrization of the quark mixing matrix. Notice that the fact that the latest SK data yield the allowed values of  $\Delta m_{atm}^2$  which are somewhat lower than the previous ones leads to slightly higher than before allowed values of  $|U_{e3}|^2$ .

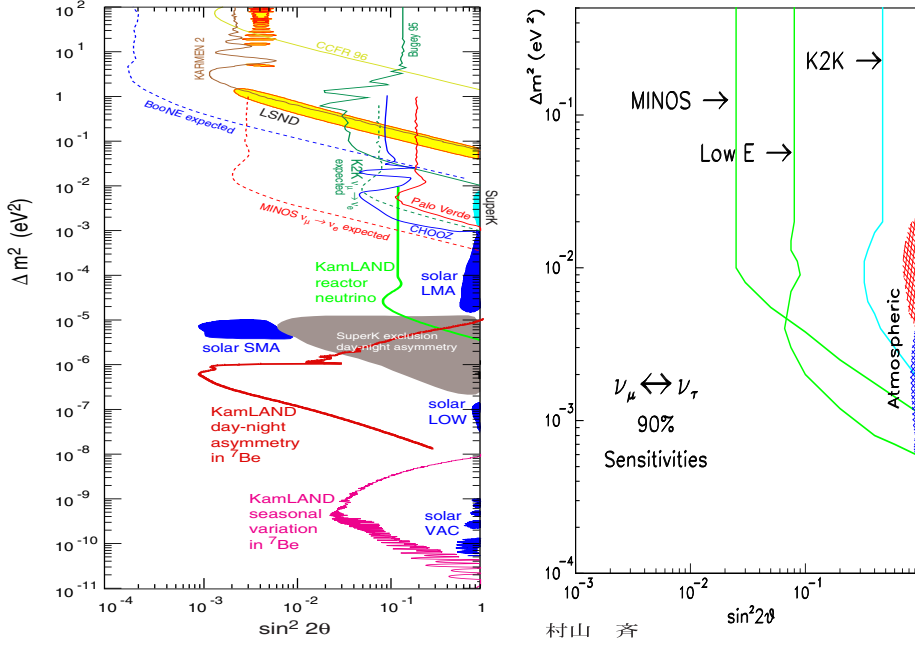


Figure 8. Left panel: results of the present and sensitivities of future  $\nu_e \leftrightarrow \nu_\mu$  oscillations searches (90% c.l.). The plot by H. Murayama. Right panel: sensitivities of MINOS and K2K long baseline experiments [41].

LSND allowed region which is presently not excluded is a narrow strip with  $\sin^2 2\theta \simeq 1 \times 10^{-3} - 4 \times 10^{-2}$  and  $\Delta m^2 \simeq 0.2 - 2 \text{ eV}^2$ .

The existing neutrino anomalies (solar neutrino problem, atmospheric neutrino anomaly and the LSND result), if all interpreted in terms of neutrino oscillations, require three different scales of mass squared differences:  $\Delta m_{\odot}^2 \lesssim 10^{-4} \text{ eV}^2$ ,  $\Delta m_{atm}^2 \sim 10^{-3} \text{ eV}^2$  and  $\Delta m_{LSND}^2 \gtrsim 0.2 \text{ eV}^2$ . This is only possible with four (or more) light neutrino species. The fourth light neutrino cannot be just the 4th generation neutrino similar to  $\nu_e$ ,  $\nu_\mu$  and  $\nu_\tau$  because this would be in conflict with the experimentally measured width of  $Z^0$  boson [see eq. (4)]. It can only be an electroweak singlet (sterile) neutrino. Therefore the LSND result, if correct, would imply the existence of a light sterile neutrino.

Out of all experimental evidences for neutrino oscillations, the LSND result is the only one that has not yet been confirmed by other experiments. It is therefore very important to have it independently checked. This will be done by the MiniBooNE (first phase of BooNE) experiment at Fermilab [42]. MiniBooNE will be capable of observing both  $\nu_\mu \rightarrow \nu_e$  appearance and  $\nu_\mu$  disappearance. If the LSND signal is due to  $\nu_\mu \rightarrow \nu_e$  oscillations, MiniBooNE is expected to detect an excess of several hundred of  $\nu_e$  events

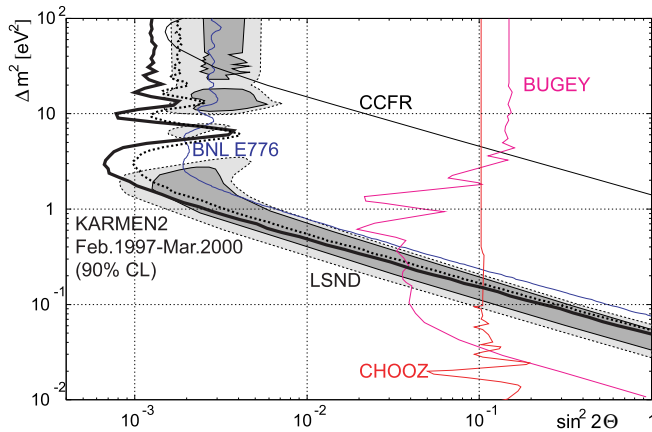


Figure 9. LSND allowed parameter region for  $\bar{\nu}_\mu \rightarrow \bar{\nu}_e$  oscillations (shaded areas) along with KARMEN, BNL E776, CCFR, CHOOZ and Bugey exclusion regions [40].

during its first year of operation, establishing the oscillation signal at  $8\sigma$  to  $10\sigma$  level (see the left panel of fig. 8). If this happens, the second detector will be installed, with the goal to accurately measure the oscillation parameters. MiniBooNE will begin taking data in 2002.

A number of long baseline accelerator neutrino experiments have been proposed to date. They are designed to independently test the oscillation interpretation of the results of the atmospheric neutrino experiments, accurately measure the oscillation parameters and to (possibly) identify the oscillation channel. The first of these experiments, K2K (KEK to Super-Kamiokande), started taking data in 1999. It has a baseline of 250 km, average neutrino energy  $\langle E \rangle \simeq 1.4$  GeV and is looking for  $\nu_\mu$  disappearance. K2K should be able to test practically the whole region of oscillation parameters allowed by the SK atmospheric neutrino data except perhaps the lowest- $\Delta m^2$  part of it (see fig. 8). The data collected from June 1999 to June 2000 ( $2.6 \times 10^{19}$  protons on target) have been reported [43]. The observed number of fully contained  $\mu$ -like event is 27 with a background of less than  $10^{-3}$  events. This has to be compared with the expected number  $40.3^{+4.7}_{-4.6}$  assuming no neutrino oscillations. The observed deficiency of  $\mu$ -like events disfavors the no-oscillation hypothesis at  $2\sigma$  level and supports the neutrino oscillation interpretation of the SK atmospheric neutrino data. However, more data have to be accumulated before definitive conclusions can be drawn.

Two other long baseline projects, NuMI - MINOS (Fermilab to Soudan mine in the US) [44] and CNGS (CERN to Gran Sasso in Europe) [45], each with the baseline of 730 km, will be sensitive to smaller values of  $\Delta m^2$  and should be able to test the whole allowed region of SK (fig. 8). MINOS

will look for  $\nu_\mu$  disappearance and spectrum distortions due to  $\nu_\mu \rightarrow \nu_x$  oscillations. It may run in three different energy regimes – high, medium and low energy ( $\langle E \rangle \simeq 12, 6$  and  $3$  GeV, respectively). MINOS is scheduled to start taking data in 2003. CERN to Gran Sasso ( $\langle E \rangle \simeq 17$  GeV) will be an appearance experiment looking specifically for  $\nu_\mu \rightarrow \nu_\tau$  oscillations. It will also probe  $\nu_\mu$  disappearance and  $\nu_\mu \rightarrow \nu_e$  appearance. At the moment, two detectors have been approved for participation in the experiment – OPERA and ICARUS. The whole project was approved in December of 1999 and the data taking is planned to begin in 2005 [46].

Among widely discussed now future projects are neutrino factories – muon storage rings producing intense beams of high energy neutrinos. In addition to high statistics studies of neutrino interactions, experiments at neutrino factories should be capable of measuring neutrino oscillation parameters with high precision and probing the subdominant neutrino oscillation channels, matter effects and CP violation effects in neutrino oscillations [47].

## 6. Phenomenological neutrino mass matrices

As was discussed before, one needs at least four light neutrino species to accommodate the data of all neutrino experiments, which would imply the existence of a light sterile neutrino. If, however, the LSND result, which has not yet been independently confirmed, is left out, one can describe all the data with just three usual neutrinos  $\nu_e$ ,  $\nu_\mu$  and  $\nu_\tau$ . We shall discuss here 3-neutrino schemes and only briefly comment on the 4-neutrino schemes.

As follows from the analyses of solar and atmospheric neutrino data, there are two distinct mass squared difference scales in the three neutrino framework,  $\Delta m_{atm}^2 \sim 10^{-3} \text{ eV}^2$  and  $\Delta m_\odot^2 \lesssim 10^{-4} \text{ eV}^2$ . The hierarchy  $\Delta m_{atm}^2 \gg \Delta m_\odot^2$  means that one of the three neutrino mass eigenstates (which we denote  $\nu_3$ ) is separated by the larger mass gap from the other two. One then has to identify  $|\Delta m_{31}|^2 \simeq |\Delta m_{32}|^2 = \Delta m_{atm}^2$ ,  $|\Delta m_{21}|^2 = \Delta m_\odot^2$ .

We know already from the 2-flavour analysis that  $\nu_\mu \leftrightarrow \nu_\tau$  should be the main channel of oscillations whereas  $\nu_e \leftrightarrow \nu_{\mu,\tau}$  oscillations can only be present as the subdominant channels. In the 3-flavour framework this means that the element  $U_{e3}$  of the lepton mixing matrix  $U_{ai}$  is small. This is in accord with the CHOOZ limit (19). The smallness of  $U_{e3}$  means that the  $\nu_\mu \leftrightarrow \nu_\tau$  and  $\nu_e \leftrightarrow \nu_{\mu,\tau}$  oscillations approximately decouple, and the 2-flavour analysis gives a good first approximation. In terms of the standard parametrization of the lepton mixing matrix, the mixing angle describing the main channel of the atmospheric neutrino oscillations is  $\theta_{23}$ , and its best-fit value following from the SK data is  $45^\circ$ . This fact and the smallness of  $|U_{e3}| \equiv \sin \theta_{13}$  mean that the mass eigenstate  $\nu_3$  mainly consists of the

flavour eigenstates  $\nu_\mu$  and  $\nu_\tau$  with approximately equal weights, while the admixture of  $\nu_e$  to this state is small or zero. Together with the unitarity of the lepton mixing matrix, this implies that solar neutrino oscillations, which are governed by the mixing angle  $\theta_{12}$ , transform the solar  $\nu_e$  into a superposition of  $\nu_\mu$  and  $\nu_\tau$  with equal or almost equal weights. This holds irrespective of whether the solution of the solar neutrino problem is LMA, SMA, LOW or VO.

With  $\Delta m_{\odot}^2 \ll \Delta m_{atm}$  there are three possible types of neutrino mass ordering. The first is the “normal”, or direct hierarchy  $m_1, m_2 \ll m_3$ ; the second possibility is an inverted mass hierarchy  $m_3 \ll m_1 \simeq m_2$ . The present-day data do not discriminate between the normal and inverted hierarchies; such a discrimination may become possible in future if the earth’s matter effects in atmospheric or long baseline  $\nu_e \leftrightarrow \nu_\mu$  or  $\nu_e \leftrightarrow \nu_\tau$  oscillations are observed. Finally, neutrinos may be quasi-degenerate in mass, with only their mass squared differences being hierarchical. Direct neutrino mass measurements allow the average neutrino mass as large as a few eV (provided that the  $2\beta 0\nu$  constraint (8) is satisfied). In that case neutrinos could constitute a noticeable fraction of the dark matter of the universe (hot dark matter).

The experimental information on the neutrino masses and lepton mixing angles allows one to reconstruct the phenomenologically allowed forms of the neutrino mass matrix  $M_\nu$ . For example, assuming  $\theta_{23} = \pi/4$  and the direct mass hierarchy, one finds (in the basis in which the mass matrix of charged leptons is diagonal) a simple zeroth order texture for  $M_\nu$  which is the first matrix on the r.h.s. of eq. (20):

$$M_\nu \propto \begin{pmatrix} 0 & 0 & 0 \\ 0 & 1 & 1 \\ 0 & 1 & 1 \end{pmatrix} \Rightarrow \begin{pmatrix} \kappa & \varepsilon & \varepsilon' \\ \varepsilon & 1 + \delta - \delta' & 1 - \delta \\ \varepsilon' & 1 - \delta & 1 + \delta + \delta' \end{pmatrix}. \quad (20)$$

It yields  $\Delta m_{\odot}^2 \equiv \Delta m_{21}^2 = 0$ , and so to get a realistic mass matrix one has to fill in zero entries with small nonzero terms and also to slightly perturb the large entries, i.e. to modify  $M_\nu$  as shown in eq. (20) (the parameters  $\kappa$ ,  $\varepsilon$ ,  $\varepsilon'$ ,  $\delta$  and  $\delta'$  are assumed to be small). Similarly, one can find zeroth order textures for the inverted mass hierarchy:

$$M_\nu \propto \begin{pmatrix} \pm 2 & 0 & 0 \\ 0 & 1 & -1 \\ 0 & -1 & 1 \end{pmatrix}; \quad \begin{pmatrix} 0 & 1 & \pm 1 \\ 1 & 0 & 0 \\ \pm 1 & 0 & 0 \end{pmatrix}, \quad (21)$$

from which realistic mass matrices can be obtained through the modifications analogous to those in eq. (20). The small entries of the neutrino mass matrices have to satisfy certain constraints [48].

The fact that at least one of the lepton mixing angles,  $\theta_{23}$ , is large came as a surprise to many people. The general expectations were that the mixing angles in the leptonic sector are small, as they are in the quark sector. The smallness of the quark mixing angles, i.e. the fact that the CKM matrix  $V = V_u^\dagger V_d$  is close to the unit matrix, implies  $V_u \simeq V_d$ . This can be understood as an indication that the up-type and down-type quarks get their masses in a similar way, so that the unitary matrices  $V_u$  and  $V_d$  of left-handed rotations that diagonalize the quark mass matrices  $M_u$  and  $M_d$  are similar.

The lepton mixing matrix is also a product of two unitary matrices, the matrices of left-handed rotations of the mass matrices of charged leptons and neutrinos:  $U = U_l^\dagger U_\nu$ . However, charged leptons and neutrinos are different in a very important way: the former are charged and can only be Dirac particles whereas the latter are neutral and can also be Majorana particles. Majorana particles can get their masses in a way which is very different from that of Dirac particles. In particular, neutrino masses can be generated by the seesaw mechanism or radiatively. Thus, there are no *a priori* reasons to expect that  $U_l \simeq U_\nu$  and that the lepton mixing is small. Actually, the fact that  $\theta_{23}$  is large may be an indirect indication that neutrinos are Majorana particles.

We don't know yet if the mixing angle  $\theta_{12}$  that governs the solar neutrino oscillations is large or small, though the current data seem to favour large values of  $\theta_{12}$ . At the same time, we know that the mixing angle  $\theta_{13}$  is relatively small (or may be very small), see eq. (19). This mixing angle can be probed in future long baseline experiments which are going to study  $\nu_e \leftrightarrow \nu_{\mu,\tau}$  appearance, earth matter effects on neutrino oscillations and CP violation in the leptonic sector. It can also be probed in reactor neutrino experiments and through the detection of neutrinos from a future galactic supernova. CERN to Gran Sasso (and possibly Fermilab to Soudan mine) experiments are expected to be able to measure the values of  $|U_{e3}|^2$  of the order of  $10^{-2}$  [45], reactor experiments could probe the values of  $|U_{e3}|^2$  down to  $\sim 3 \times 10^{-3}$  [49], supernova neutrino detection could have an order of magnitude better sensitivity [50], and neutrino factories may be able to probe as small values of  $|U_{e3}|^2$  as a few  $\times 10^{-5}$  [47].

Can we understand the fact that  $|U_{e3}| = \sin \theta_{13}$  is small even though  $\theta_{23}$  and probably also  $\theta_{12}$  are large? And can we get at least a rough idea of how small  $|U_{e3}|$  actually is? The latter would be of great importance for future long baseline experiments.

One can obtain an order of magnitude estimate of  $|U_{e3}|$  if one assumes that there is no fine tuning between the elements (12) and (13) of the neutrino mass matrix  $M_\nu$  (in the notation of eq. (20), between  $\varepsilon$  and  $\varepsilon'$ ). Then, neglecting possible leptonic CP violation effects, one finds the following

approximate relation between  $U_{e3}$ ,  $\theta_{12}$ ,  $\Delta m_{\odot}^2$  and  $\Delta m_{atm}^2$  [51]:

$$U_{e3}^2 \simeq \frac{1}{4} \cdot \frac{\tan^2 2\theta_{12}}{(1 + \tan^2 2\theta_{12})^{1/2}} \cdot \frac{\Delta m_{\odot}^2}{\Delta m_{atm}^2}. \quad (22)$$

This expressions provides an explanation of the smallness of  $U_{e3}$ : it is a consequence of the hierarchy  $\Delta m_{\odot}^2 \ll \Delta m_{atm}^2$ . Since the value of  $\Delta m_{atm}^2$  is fixed (within a factor of 3 or so) by the SK atmospheric neutrino data, the actual value of  $U_{e3}$  depends on the solution of the solar neutrino problem. In particular, for the LMA solution (which is currently the preferred one) eq. (22) predicts rather large values of  $U_{e3}$  which may be just below the CHOOZ limit (19). This means that  $U_{e3}$  may be measured soon! One should, however, keep in mind that eq. (22) gives only plausible values of  $U_{e3}$  as its predictions are crucially based on the assumption of no fine tuning between the elements  $\varepsilon$  and  $\varepsilon'$  of the neutrino mass matrix (20). Such a fine tuning may, actually, be there and be natural if it is enforced by a flavour symmetry.

Four-neutrino schemes can be analyzed similarly to the 3-neutrino case. The data allow essentially two 2+2 schemes. In each of these schemes there are two pairs of nearly degenerate mass eigenstates separated by large  $\Delta m_{LSND}^2$ . The mass splittings between the components of the quasi-degenerate pairs are  $\Delta m_{\odot}^2$  and  $\Delta m_{atm}^2$ . There are also 3+1 schemes in which one of the mass eigenstates is separated by the large  $\Delta m_{LSND}^2$  from the rest of the states. The most attractive 3+1 scheme is the one in which the lone mass eigenstate is predominantly the sterile neutrino; in this scheme the 3-flavour dynamics of solar and atmospheric neutrino oscillations is only slightly perturbed. Until recently, this scheme has been considered experimentally disfavoured (compared to the 2+2 schemes), but with the recent SK data the situation has changed. In 2+2 schemes the total contribution of sterile neutrinos to oscillations of solar and atmospheric neutrinos is equal to unity, so the fact that SK disfavours the pure active to sterile oscillations of *both* atmospheric and solar neutrinos makes the 2+2 schemes less plausible. At the same time, the recently reported new analysis of the LSND data [39] has shifted the allowed parameter space towards smaller mixing angles, which improves the fit within the 3+1 scheme. Therefore the 3+1 scheme in which the lone mass eigenstate is predominantly  $\nu_s$  is now also acceptable [36, 52, 53]. Different 3+1 schemes can also fit the data [54]. Other recent discussions of the  $4\nu$  schemes can be found in [21, 34, 55, 56]).

The neutrino mass matrix textures can provide us with a hint of the symmetries or dynamics underlying the theory of neutrino mass. With the forthcoming data from future neutrino experiments, it may eventually become possible to uncover the mechanism of the neutrino mass generation, which may hold the clue to the general fermion mass problem.

It is very likely that in a few years from now new experiments will bring us the answers to many questions about neutrinos and finally allow us to solve the solar neutrino problem. Neutrinos may also bring us new surprises, as they did many times in the past.

This work was supported by Fundação para a Ciência e a Tecnologia through the grant PRAXIS XXI/BCC/16414/98 and also in part by the TMR network grant ERBFMRX-CT960090 of the European Union.

## References

1. Super-Kamiokande Collaboration, Fukuda, Y., *et al.* (1998) *Phys. Rev. Lett.* **81**, 1562.
2. Smirnov, A.Yu., hep-ph/9901208.
3. Altarelli, G. and Feruglio, F., hep-ph/9905536.
4. Tanimoto, M., hep-ph/9910261.
5. Mohapatra, R.N., hep-ph/9910365.
6. Fritzsche, H. and Xing, Z.-z., hep-ph/9912358.
7. Barr, S.M. and Dorsner, I., hep-ph/0003058.
8. Bilenky, S.M., Giunti, C. and Grimus, W. (1999) *Prog. Part. Nucl. Phys.* **43**, 1.
9. Akhmedov, E.Kh., hep-ph/0001264.
10. Lobashev, V.M., Talk given at the *XIX Intern. Conf. on Neutrino Phys. and Astrophys. "Neutrino 2000"*, Sudbury, Canada, June 16 – 21, 2000. Transparencies at <http://nu2000.sno.laurentian.ca/>
11. Weinheimer, C., Talk given at *Neutrino 2000*, see ref. [10].
12. Particle Data Group, Groom, D.E. *et al.* (2000) *Eur. Phys. J.* **C15**, 1.
13. Roney, J.M., Talk given at *Neutrino 2000*, see ref. [10].
14. Okada, K. for the DONUT Collaboration, talk at Neutrino Oscillations Workshop NOW2000, Conca Specchiulla, Italy, Sept. 9-16, 2000. Transparencies at <http://www.ba.infn.it/~now2000/views/slides/>
15. Sarkar, S., astro-ph/9903183.
16. Baudis, L. *et al.*, Heidelberg-Moscow Collaboration (1999) *Phys. Rev. Lett.* **83**, 41.
17. Ejiri, H., Talk given at *Neutrino 2000*, see ref. [10].
18. Sobel, H., Talk given at *Neutrino 2000*, see ref. [10]; Learned, J.G., hep-ex/0007056.
19. Kajita, T., Talk given at NOW2000, see ref. [14].
20. The Super-Kamiokande Collaboration, Fukuda, S. *et al.*, hep-ex/0009001.
21. Fogli, G.L., Lisi, E. and Marrone, A., hep-ph/0009299.
22. CHOOZ Collaboration, Apollonio, M. *et al.*, *Phys. Lett.* **B466**, 415.
23. Fogli, G.L. *et al.*, hep-ph/0009269.
24. Gonzalez-Garcia, M.C. *et al.*, hep-ph/0009350.
25. Fogli, G.L. *et al.* (1999) *Phys. Rev.* **D60**, 053006.
26. Barger, V. *et al.* (1999) *Phys. Lett.* **B462**, 109.
27. Geiser, A. for the MONOLITH Collaboration, hep-ex/0008067.
28. Bahcall, J.N., <http://www.sns.ias.edu/~jnb/>
29. Krastev, P.I., Talk given at NOW2000, see ref. [14].
30. Mikheyev, S.P. and Smirnov, A.Yu. (1985) *Sov. J. Nucl. Phys.* **42**, 913; Wolfenstein, L. (1978) *Phys. Rev.* **D17**, 2369.
31. Suzuki, Y., Talk given at *Neutrino 2000*, see ref. [10].
32. Recent fits of the solar neutrino data can also be found in Gonzalez-Garcia, M.C. and Peña-Garay, C., hep-ph/0009041; talks given by Montanino, D. and Palazzo, A. at NOW2000, see ref. [14]; Gonzalez-Garcia, M.C. *et al.*, ref. [24].
33. Fogli, G.L., Lisi, E. and Montanino (1996) *Phys. Rev.* **D54**, 2048.
34. Giunti, C., Gonzalez-Garcia, M.C. and Peña-Garay, C. (2000) *Phys. Rev.* **D62**, 013005.

35. de Gouvêa, A., Friedland, A. and Murayama, H. (2000) *Phys. Lett.* **B490**, 125.
36. Smirnov, A.Yu., Talk given at *Neutrino 2000*, see ref. [10]; hep-ph/0010097.
37. McDonald, A.B. for the SNO Collaboration, Talk given at *Neutrino 2000*, see ref. [10]; hep-ex/0011025.
38. For recent discussions see de Gouvêa, A., Friedland, A. and Murayama, H., hep-ph/9910286; Fogli, G.L. *et al.* (2000) *Phys. Rev.* **D61**, 073009.
39. Mills, G. for the LSND Collaboration, Talk given at *Neutrino 2000*, see ref. [10].
40. Eitel, K. for the KARMEN Collaboration, Talk given at *Neutrino 2000*, see ref. [10]; hep-ex/0008002.
41. Conrad, J., hep-ex/9811009.
42. Bazarko, A.O. for the MiniBooNE Collaboration, Talk given at *Neutrino 2000*, see ref. [10]; hep-ex/0009056.
43. Boyd, S, hep-ex/0011039.
44. Wojcicki, S. for the MINOS Collaboration, Talk given at *Neutrino 2000*, see ref. [10].
45. Rubbia, A, Talk given at *Neutrino 2000*, see ref. [10]; hep-ex/0008071.
46. For numerous links to various solar, atmospheric, reactor, accelerator and other neutrino experiments see the Neutrino Oscillation Industry Web page maintained by M. Goodman, [http://www.hep.anl.gov/ndk/hypertext/nu\\_industry.html](http://www.hep.anl.gov/ndk/hypertext/nu_industry.html)
47. See, e.g., Albright, C. *et al.*, hep-ex/0008064 and references therein.
48. Akhmedov, E.Kh. (1999) *Phys. Lett.* **B467**, 95.
49. Mikaelian, L.A., Talk given at *Neutrino 2000*, see ref. [10]; hep-ex/0008046.
50. Dighe, A.S. and Smirnov, A.Yu. (2000) *Phys. Rev.* **D62**, 033007.
51. Akhmedov, E.Kh., Branco, G.C. and Rebelo, M.N. (2000) *Phys. Rev. Lett.* **84**, 3535.
52. Peres, O.L.G., and Smirnov, A.Yu., hep-ph/0011054.
53. Barger, V. *et al.*, hep-ph/0008019.
54. Giunti, C. and Laveder, M., hep-ph/0010008.
55. Yasuda, O., hep-ph/0006319.
56. Gonzalez-Garcia, M.C. and Peña-Garay, C., in ref. [32].